



Published in final edited form as:

*Minim Invasive Ther Allied Technol.* 2006 ; 15(2): 101–113. doi:10.1080/13645700600674179.

## Interventional robotic systems: Applications and technology state-of-the-art

KEVIN CLEARY<sup>1</sup>, ANDREAS MELZER<sup>4</sup>, VANCE WATSON<sup>1</sup>, GERNOT KRONREIF<sup>3</sup>, and DAN STOIANOVICI<sup>2</sup>

<sup>1</sup>Imaging Science and Information Systems (ISIS) Center, Department of Radiology, Georgetown University Medical Center, Washington, DC, USA

<sup>2</sup>URobotics Laboratory, Urology Department, Johns Hopkins Medicine, Baltimore, Maryland, USA

<sup>3</sup>Mechatronic Automation Systems - Robotics Lab, ARC Seibersdorf research, Seibersdorf, Austria

<sup>4</sup>Institute for Innovative Technologies and Management in Medicine INSITE med. & Dept. of Physical Engineering, University of Applied Sciences, Gelsenkirchen, Germany, & St. Mary's Hospital Buer, Dept of Radiology, Gelsenkirchen Buer, Germany

### Abstract

Many different robotic systems have been developed for invasive medical procedures. In this article we will focus on robotic systems for image-guided interventions such as biopsy of suspicious lesions, interstitial tumor treatment, or needle placement for spinal blocks and neurolysis. Medical robotics is a young and evolving field and the ultimate role of these systems has yet to be determined. This paper presents four interventional robotics systems designed to work with MRI, CT, fluoroscopy, and ultrasound imaging devices. The details of each system are given along with any phantom, animal, or human trials. The systems include the AcuBot for active needle insertion under CT or fluoroscopy, the B-Rob systems for needle placement using CT or ultrasound, the INNOMOTION for MRI and CT interventions, and the MRBot for MRI procedures. Following these descriptions, the technology issues of image compatibility, registration, patient movement and respiration, force feedback, and control mode are briefly discussed. It is our belief that robotic systems will be an important part of future interventions, but more research and clinical trials are needed. The possibility of performing new clinical procedures that the human cannot achieve remains an ultimate goal for medical robotics. Engineers and physicians should work together to create and validate these systems for the benefits of patients everywhere.

### Keywords

Medical robotics; minimally invasive procedures; interventional robots; image-guided interventions; MR-guided interventions

---

© 2006 Taylor & Francis

Correspondence: K. Cleary, Imaging Science and Information Systems (ISIS) Center, Department of Radiology, Georgetown University Medical Center, 2115 Wisconsin Ave., Suite 603, Washington, DC 20007. Fax: +1-202-784-3479. cleary@georgetown.edu.

## Introduction

Many different robotic systems have been developed for invasive medical procedures. In this article we will focus on robotic systems for minimally invasive interventions such as biopsy of suspicious lesions or needle placement for spinal blocks. According to the Robotic Institute of America, a robot is “a reprogrammable, multifunctional manipulator designed to move materials, parts, tools, or other specialized devices through various programmed motions for the performance of a variety of tasks.” For our purposes, this definition fits most medical robotics systems fairly well, in that they are typically mechanical manipulators with rigid links connected by joints that allow relative motion from one link to another (1).

Medical robotics is a relatively young field, with the first recorded medical application of a robot occurring in 1985 (2). Unlike factory robotics, in which virtually all operations are now automated and the use of robotics is widespread, medical robotics is still a niche field. While medical robots have been applied in many fields such as neurosurgery, orthopedics, and urology, they are not the standard of care in any field and in fact very limited market penetration has occurred. This limited use is no doubt due to the many challenges that need to be overcome in developing a robotic system for a medical application. In particular, safety is an overriding concern and must be considered from the start in any medical robotic system. Note that in the factory, we do everything we can to keep people away from robots, but in the medical environment many robotic systems are designed to work with people nearby, and all medical robotics systems must ensure safe operation with a patient in the workspace of the robot. Despite these challenges, we believe that medical robotic systems have a place in minimally invasive procedures, and this article describes several systems developed by the authors for this purpose.

There are many other robotic systems which have been developed and there are several review articles that have been written in the past few years such as (3-6). In particular, there are two systems that are currently used in clinical practice that should be mentioned here. The first system is the da Vinci H from Intuitive Surgical (Sunnyvale, California, USA) which functions along the line of a master – slave telemanipulator for endoscopic surgical procedures developed in the early 1990’s (7). The da Vinci consists of the surgeon’s viewing and control console, a control unit, and a three-arm surgical manipulator (8). While the initial application of the system was cardiac surgery, a recent focus of the company has been on urological surgery, specifically minimally invasive prostatectomy. According to the manufacturer, about 400 systems have been installed to date. The second system is the CyberKnife H from Accuray (Sunnyvale, California, USA) for stereotactic radiosurgery. The CyberKnife consists of a lightweight linear accelerator, a KUKA robot, paired orthogonal x-ray imagers, and a treatment couch (9). The system was originally developed to treat tumors in the brain and spine, but is now FDA approved to treat lesions anywhere in the body including the lung and pancreas. According to the manufacturer, over 100 systems have been sold to date.

The article is organized as follows. In a section constituting the bulk of the article, we describe four interventional systems designed to work with MRI, CT, fluoroscopy, and ultrasound imaging devices. The details of each system are given along with any phantom, animal, or human trials. The paper concludes with a presentation of some technology issues followed by a discussion and summary.

### Interventional robotics systems

In this section, four interventional robotics systems which were developed by the authors will be presented. Table I lists the system name, institution where the system was developed, the status (phantom, animals, clinical trial), and the imaging modality used. Note that these

systems are representative examples of the state of the art in interventional robotics. There are other systems that have been built and the reader is referred to the review articles listed earlier for more details.

## Acubot

The AcuBot (10) robot presents a modular structure of several functionally distinctive components that have been developed over the past five years in the URobotics Laboratory at Johns Hopkins Medical Institutions (Baltimore, USA). The AcuBot incorporates the original PAKY (percutaneous access of the kidney) radiolucent needle driver (11), a RCM (remote center of motion) module capable of needle orientation (12), an XYZ Cartesian stage for translational positioning of the needle tip, and a passive positioning arm (S-arm) mounted onto a bridge frame.

Figure 1 shows two views of the robot mounted on a CT scanner. The base of the robot (2) provides a bridge-like structure over the table. The robot has a total of six active degrees of freedom (DOF) configured for decoupled positioning, orientation, and instrument insertion. The instrument [7] is loaded in PAKY [6], which is an active radiolucent needle driver (T translation). PAKY is held by the RCM (11) module [5]. This module is capable of precisely orienting the instrument about two nearly perpendicular directions (Rx and Rz) coincident at the RCM point, thus allowing a pivoting motion about that point. The RCM is supported by a passive positioning arm [4], called the S-ARM, with seven DOF (S1 spherical, R revolute, S2 spherical). The arm can be positioned and rigidly locked from a single lever. The base of the arm [4] is mounted in a 3DOF Cartesian stage [3], the XYZ module (Tx, Ty, and Tz translations). The user interface consists of a 15" resistive touch screen [8], a two-axis joystick, a switch panel [10], and an emergency stop button [11]. These components are mounted on the front side of the bridge. A speaker [9] and the cable connector [12] are located on its back side.

**Needle registration and clinical studies in CT scanners**—The method is based on aligning the procedure needle held by the robot with the laser markers of the CT scanner. The robot can then automatically orient the needle toward a target selected in a CT slice. The skin entry point and target location may be contained in different slices. Needle insertion may then be performed under joystick control or automatically under CT fluoroscopy (CTF) monitoring by the physician.

This method showed an experimental accuracy of <1 mm in-slice and 1.5 mm for out-of-slice targets. Four clinical cases of kidney and spine biopsy and RF ablation and a nephrostomy tube placement were successfully performed with no complications (13). These cases demonstrated a significant improvement over the manual method, in which the needle is typically restricted to the CTF plane so that the needle can always be seen by the physician.

Another study (14) with the same robotic system found the *in-vitro* accuracy of the robot to be 0.6° angular and 1.65 mm linear. The clinical study included ten percutaneous core biopsies (7 kidney, 2 lung, 1 liver), 11 RF ablations (9 kidney, 2 spine), one nephrostomy tube placement, and one neobladder access. In four cases, the target was not met adequately, and fine-tuning adjustment with the joystick was required to reach the target. In all cases, however, the study showed that the use of the robot reduced radiation exposure for the patient and medical personnel.

**Clinical trial for nerve blocks under fluoroscopy**—After cadaver studies using the robot to precisely position a needle in the lumbar spine were successfully completed (15) in the Department of Radiology at Georgetown University, a randomized clinical trial of 20

patients undergoing nerve and facet blocks was approved by the FDA and the local institutional review board. The procedure was done following the usual clinical practice except the robot was used to position, orient, and drive the needle under physician control. A/P fluoroscopy was used to position and orient the needle, and lateral fluoroscopy was used to monitor the depth of insertion.

The robot was mounted on the interventional table using a custom-designed locking mechanism. The robot was positioned initially near the skin entry point by loosening the passive gross positioning mechanism and moving the needle driver end of the robot by hand. Once this initial position had been attained, the mechanism was locked and the robot was switched to operate by physician control using the joystick.

The study was completed by a single fellowship trained interventional neuroradiologist at Georgetown University Hospital using a Siemens Neurostar biplane fluoroscopy system. The standard manual technique was used on ten patients and the robotic device was used on ten patients. The patients ranged in age from 30 to 70 years. The spine levels were from S-1 to L-5. No complications were observed in the study. One of the patients in the robotics arm had to be converted to a manual procedure due to slippage of the needle driver. This conversion was done without difficulty or complications.

There were two outcome measures:

- accuracy of needle placement, and
- pain relief.

Accuracy of needle placement was determined as follows. Before the interventionalist began placing the needle, both an A/P and lateral image of the patient were obtained. The interventionalist would then annotate each image with an arrow to indicate the desired target location of the needle (the interventionalist was not blinded as to manual/robotic technique as this was not practical). After the needle was placed, an A/P and lateral image was again obtained. The two sets of images were compared to determine the distance between the intended location of the needle and the actual location of the needle. Pain relief was measured using a visual-analog scale, with 0 representing no pain and 10 representing excruciating pain.

The results to date show that it is feasible to use a joystick controlled robot for nerve and facet blocks. While this was a pilot study and not enough data was gathered for statistical significance, some general trends can be observed. The mean accuracy in the robot (1.105 mm) and manual (1.238 mm) is about the same. Therefore, it appears that the robot is capable of accurate needle placement.

As expected, the pain score post-treatment was significantly less than the pain score pre-treatment in both the robot and manual arms. In the robot arm, pain scores fell from a mean of 6.3 pre-treatment to 1.8 post-treatment. In the manual arm, pain scores fell from 6.0 pre-treatment to 0.9 post-treatment. Patients had to sign an informed consent form and were generally receptive to the use of the robot.

**B-Rob systems – ARC Seibersdorf Research:** Robotic systems for CT and ultrasound-guided biopsies have been developed by the robotics laboratory of ARC Seibersdorf Research in Austria. The two systems developed by this group are presented here.

**Prototype Biopsy Robot I (B-RobI)**—The first prototype biopsy robot was called B-RobI and was a seven degree of freedom (DOF) stand-alone robot system integrated on a mobile rack (16). The biopsy instrument is positioned at the skin entry point by a 4-DOF

gross positioning system consisting of three Cartesian linear axes together with one additional rotational link for a rough orientation of the needle. For final orientation of the needle the robot is equipped with a “Needle Positioning Unit” (NPU) consisting of two linear DOFs which move two parallel carbon “fingers” connected by spherical links. Another linear DOF with a limited stroke of 50mm can move the entire NPU toward the skin entry point in a safe approach movement, i.e. with minimal velocity and force. The needle orientation stage is thus strictly decoupled from movement of any axis of the gross positioning system. A remote center of motion (“pivot point”) for angulation of the needle is maintained by the kinematic structure of the NPU as another safety measure during the intervention.

The robot system is controlled by two industrial PCs. One PC provides high-level control of the robot system and a second PC handles the interface to the optical tracker system (Polaris, Northern Digital, Bakersfield, CA, USA) as well as the planning and monitoring software. This PC also includes a video capture card (WinTV-PCI-FM 718, Hauppauge) for grabbing images from an ultrasound probe or the CT monitor to support planning of an intervention. After acquisition of images of the target region, the physician selects the desired skin entry point as well as the target point. With that information the relevant data (angulation, distance to the target lesion) are calculated and automatically sent to the robot controller via TCP/IP socket connection. Using the graphical user interface (GUI) of the planning software, the virtual trajectory of the biopsy can be viewed in all CT-slices involved to verify the intervention path. After planning of the intervention, the robot can be moved towards its final position by a coordinated motion of the axes. The gross positioning unit can then be locked if desired. The NPU is then moved to the skin entry point under very controlled conditions (at low speed and with limited distance) and the needle can be manually inserted.

The performance of the complete system has been extensively evaluated in a series of in vitro tests using a needle-penetrable phantom (17-19). Peas (mean diameter =  $9.4 \pm 0.7$  mm) were embedded as targets within a custom-made gel-phantom. Based on the intervention plan, the NPU was commanded to the desired skin entry point to provide guidance for a 17-gauge coaxial puncture needle and an 18-gauge long biopsy needle. After manual needle insertion, sample harvesting was performed by means of an automated biopsy device (Magnum Core high speed; 22-mm excursion). The distance between the actual needle tract and the centre of the target was evaluated in two orthogonal axes using ultrasonography – the length of the harvested biopsy specimen was also evaluated by direct measurement. Test series were performed for both US-guided biopsies (scanning head C4-2; US-System HDI-UM 9, Advanced Technology Laboratories, USA) as well as for CT-guided interventions (Multidetector CT, Siemens Somatom Sensation 16; CareVision Mode, 0.75 c 0.75, 80 kV, 160 mAs, 0.5 sec). Photographs of the CT tests are shown in Figures 4 and 5.

The system showed sufficient operational stability and accuracy for the procedures under consideration. The measured targeting accuracy ( $1.48 \text{ mm} \pm 0.62 \text{ mm}$ ) is better compared to traditional techniques by additionally combining the advantages of needle guidance and free-hand technique. Integration of the complete system on a mobile rack allows short setup time and easy installation of the system at different sites. On the other hand, the chosen approach leads to a very bulky system and to a very high grade of automation.

**Biopsy Robot II (B-RobII)**—The main goal for this new design was to transfer the concepts demonstrated from the B-RobI prototype into a practical clinical setup. The major goals for the new development were:

- a modular setup for a broad variety of clinical applications,

- a significant reduction of technical complexity (compared to the previous prototype) to reach an acceptable cost/benefit ratio for the entire system,
- easy integration to devices used in interventional radiology,
- seamless integration to clinical workflow, and
- a “plug&play” philosophy.

The mechanical architecture for the new design was based on the parallelogram mechanism already realized for the NPU of the B-RobI prototype. For easy sterilization, the two carbon “fingers” – together with the polymer bearings and the needle guideway – can be disconnected from the positioning module (i.e. the robot) by means of a rapid-change bayonet connection. The mechanical design of the device is low-profile (dimensions of one 2DOF module: WxLxH=100 mm × 150 mm × 30 mm) in order to use the system inside of the CT gantry without major restrictions. Following the general idea of modularity, different configurations are supported in order to allow simple 2DOF needle angulation (+/- 30°), 2DOF positioning (+/- 20 mm) as well as (optional) maintaining a software defined pivot point for angulation. For gross positioning of the needle entry point, the module(s) are mounted on one or two passive 7DOF multifunctional holding arm(s) (ATLAS arm, Medical Intelligence GmbH, Schwabmünchen, Germany) (Figure 6).

The robot control system was developed in-house and consists of two axis controllers for each module, a safety card which disconnects all motors from the power supply in case of an emergency stop, and a power supply module – all of which are integrated into a HF-dense 19” housing. All modules are interconnected via a standard RS485 bus system. Operation of the entire system is synchronized either via a PC (MDD certified computer or panel PC) connected to the RS485 bus or via a hand-held control unit in stand-alone operation. Thanks to this modular setup, single modules can be easily replaced and the system can be expanded easily.

Planning of the intervention is based on imaging data sets acquired immediately before an intervention. The spatial relation between the imaging space and the targeting device is either established by means of a tracker system (optical or mechanical) or via robot registration based on a CT-data set. After graphical selection of the target and manual pre-positioning of the device, the correct angulation will be set automatically by the system. During the intervention, the robotic kinematics holds the needle guide in a predefined position and orientation. However, the insertion of the needle itself will be performed manually by the physician.

The first *in vitro* trials of the system using a penetrable gel phantom (Figure 7) show that B-RobII allows image-guided positioning of a biopsy needle with high accuracy (0.66 mm ±0.27 mm). The system is easy to use and does not considerably interfere with the clinical work-flow. A risk analysis of the complete system (20) did not find any major risks. A series of quantitative evaluation studies – for both US and CT guided biopsies and for different system setups (no/ mechanical/ optical tracker; remote controlled operation) is currently in process. Beside biopsy procedures, further clinical applications are currently under evaluation at different research centers. The long-term goal of this work is to create a multi-purpose system for a broad range of percutaneous treatments, in any part of the body, using any kind of intraoperative image guidance.

**CT and MR-compatible robotic instrument guiding system INNOMOTION:** MR-guided percutaneous interventions have been clinically established with open low field MR systems (21). As the imaging quality of closed bore scanners is superior to open field system but the access to the patient is limited a fully MR-compatible assistance system

INNOMOTION (Innomedic, Herxheim & FZK Karlsruhe Germany & TH Gelsenkir) (22) was developed to provide precise and reproducible instrument positioning inside the magnet. MRI compatibility has been achieved through testing of all components and the complete system in different field strength magnets including a 1.5 T Siemens Magnetom Symphony and Philips 1.0 T Gyroscan and 1.5 T Intera magnets. Targeting precision has been determined with a mechanical FARO arm in dry lab experiments and on *ex vivo* organ models embedded in agarose gel. Targeting precision has also been evaluated during MRI guided percutaneous interventions in a porcine animal model. The system is shown in Figure 8 a and b

**Technology**—The pneumatic robotic assistance system is fully MR-compatible and consists of a robot arm which can be manipulated in six degrees of freedom. The robot arm is attached to a 260° arch that is mounted to the patient table of the scanner and can be passively prepositioned on either side of the arch at 0°, 30° and 60° to the vertical according to the region of interest (e.g. spine, liver, kidney, breast). Active positioning measurements are achieved via fiber optically coupled limit switches, along with rotational and linear incremental sensors. The kinematics of the device has been carefully optimized for use in close bore MRI scanners and the CT gantry. Piezoelectric drives were tested but due to the RF noise during MRI scanning and the risk of inductive heating of the electric power lines they were not used and pneumatic cylinders with slow motion control have been developed instead to drive all six degrees of freedom.

A module for application of coaxial probes (e.g. cannulae for biopsies, RF or Laser probes, endoscopes, etc.) provides two degrees of freedom in X and Z axes and is attached to a robotic arm with five degrees of freedom. This design assures stable positioning of the instrument within a tool center point that keeps the “invariant point of insertion” at the skin entry point.

The application module (Figure 9) for clinical use provides manual translation and rotation of the cannula. A pneumatic drive has been developed to insert the cannula in incremental steps of 1 – 20 mm. In conjunction with the two axes for movement about the tool center point (+/- 30°) the instrument trajectory can be changed to other targets without moving the robot arm or repositioning the arm on the arch. The arch is movable and can be firmly attached to the patient table of the MR system with exchangeable fittings easily adopted to other MRI platforms (Figure 10). A graphical user interface provides trajectory planning directly on the MRI images (Figure 11 e).

**Procedure technique**—The patient is placed in a predetermined position suitable for the intervention (supine, prone or lateral). The system is prepositioned and firmly attached to the table with clamps. Based on the pre-interventional images and the anatomical region of interest the table is moved using the projection of the laser vizier from the CT gantry. The robot is referenced to the coordinate system of the MR scanner using contrast-filled marker. The CT version comprises laser light sensors at the upper part of the application module for automated registration. The arm moves back and forth; it returns so that the light detectors are aligned with the laser (within +/- 0.5 mm). The laser light is switched off and the table can be moved into the gantry until the position of the laser line matches with the zero position of the Z-axis of the scanner. Planning for MRI intervention is performed by using fast gradient echo sequences in transverse, sagittal or coronal orientation. Suitable slices are selected and sent via the network in DICOM format to the computer of the robotic assist system. The insertion site and a target point are selected on the graphical user interface and the corresponding coordinates are sent to the control unit. The drives are activated and the application module is moved with the tool center point to the insertion site on the skin. The cannula can then be inserted through a guiding sleeve or along an open angle.

**Evaluation of targeting precision**—Mechanical targeting precision has been determined with a FARO arm under dry lab conditions. The MRI procedures were performed on 1.5 T Siemens Magnetom Symphony, and a Philips 1.0 T Gyroscan and 1.5 T Intera. The test were done on *ex vivo* organ models which consisted of fresh porcine kidney embedded in Agarose and Gelatine (Figure 12).

Targeting precision was also evaluated during MRI-guided percutaneous interventions in a porcine animal model under general anesthesia (Isoflurane). The animals (four 3-month old domestic pigs 30 – 40 kg) were placed prone on the patient table and a surface coil was fixed around the planned insertion site lateral to the spine. Using T1- and T2-weighted planning images, the appropriate region of interest was defined on the graphical user interface of the INNOMOTION control computer (Figure 13). The robot arm then moved and oriented the needle holder to the insertion point automatically. 20 and 22 gauge MR-compatible Titanium grade 4 cannulae (MRI Devices-Daum, Schwerin, Germany) were then manually inserted. Subsequent to an initial insertion of about 10 mm the table was repositioned in the MRI bore and control images were acquired. The precision of the insertion point and the insertion angle were determined by overlaying the pre-interventional images with the new MRI image.

The intervention was completed within the magnet from the rear opening, where an MR-compatible in-room monitor was placed. During the insertion of the needle, real-time MR images were acquired for guidance. To visualize the advancement of the cannula in the tissue fast Gradient Echoes sequences (TR=4.4 ms; TE=2.2 ms; FA 70°; TA=0.7 s) were used. At the desired region of interest (nerve root or plexus coeliacus) spin echo images were acquired for verification of the cannula position through a test bolus of contrast agent solution (NaCl/GdDTPA: 100/1litre of 0.9% saline solution). The injection was done under real-time MRI (TR=1.8 ms; TE=4.3 ms; TA=0.5–0.8sec.; FA=20°) to visualize the drug distribution. Final therapeutic injection of 10–25 ml with contrast dotted Mepivacain-hydrochlorid (Scandicain®1%, Astra – Zeneca, Wedel, Germany) was performed.

**Results and discussion**—All procedures were completed successfully including injections at the sympathetic chain, sciatic nerve and coeliac plexus. The direct MRI control allow correction of the insertion path in case of misdirection due to anatomical structures. The insertion site and the insertion angle were evaluated by manual measurement on overlays of the planning image and the subsequent MR control image (Figure 13). The position and orientation of all cannula insertions were appropriately visualized on axial MRI images. The precision of the insertion site in the axial plane was +/- 1 mm (minimum of 0.5 mm and maximum of 3 mm). The angular deviation in the transverse plane of the cannulae was +/- 1° with a minimum of 0.5° and a maximum of 3°.

Cross platform MRI compatibility can be achieved by using polymers, ceramics, pneumatic drives and optoelectronic sensors. For MRI-guided cannula interventions, as the cannula is currently advanced manually, the access is difficult if the insertion is done inside the magnet. Therefore, the direct control of the insertion under real-time MRI is recommended to allow correcting the insertion in case of misdirection of the cannula and to precisely position the tip of the cannula in the volume of interest. To ease the procedure tip tracking techniques haven been evaluated (23).

**MrBot: A fully MRI compatible robot for prostate image-guided interventions:** A new robot, MrBot (24), has been recently developed at Hopkins for fully-automated image-guided access of the prostate gland. The robot is customized for transperineal needle insertion and designed to be compatible with all known types of medical imaging equipment. This includes uncompromised compatibility with MRI scanners of the highest



field strength, size accessibility within closed-bore tunnel-shaped scanners, and clinical intervention safety.

The robot is designed to accommodate various end-effectors for different percutaneous interventions such as biopsy, serum injections, or brachytherapy. The first end-effector developed is customized for fully-automated low dose radiation seed brachytherapy.

For MRI compatibility the robot is exclusively constructed of nonmagnetic and dielectric materials such as plastics, ceramics, and rubbers and is electricity-free. The system utilizes a new type of motors specifically designed for this application, the pneumatic step motors (PneuStep) (25). These uniquely provide easily controllable precise and safe pneumatic actuation. Fiber optic encoding is used for feedback, so that all electric components are distally located outside the imager's room. A photograph of the robot on the MR scanner table is shown in Figure 14.

Motion repeatability tests performed in the MRI scanner show mean errors of 0.076 mm. The robot was found to be compatible with all types of imaging devices (25). A linear PneuStep motor was tested in a small-bore high-strength magnet (7T). This showed very precise positioning accuracy of  $27 \pm 4 \mu\text{m}$ . No problems were encountered with the operation of the PneuStep motor in the 7T MRI environment, and no image deterioration or artifacts were observed due to the presence of the device at the isocenter or its motion during imaging.

The clinical utility of the system remains to be investigated. We are currently evaluating needle insertion accuracy with *in vitro* and *ex vivo* experiments. The brachytherapy injector is very instrumental in performing these studies, because the injector can automatically deploy seed-like imaging markers. Robot precision is then estimated by comparing the actual and desired location of the deployed markers. For compatibility and minimal artifacts under MRI we use specially made ceramic markers. These do not resonate but the image clearly shows the displaced volume, very close to its real size. The robot and seed injector can perform fully automated seed deployment on any specified 3D pattern (Figure 15). Tests performed in agar showed an average seed deployment accuracy of 0.652 mm.

Experiments continue now with other *in vitro* IGI studies. An animal protocol has already been filed and approved for *in vivo* studies. An institutional review board approval was also received for human trials on robot-scanner ergonomics.

## Technical Issues

In this section the following technical issues will be briefly discussed:

- Imager compatibility
- Registration
- Patient movement and respiration
- Force feedback
- Mode of control

### Imager compatibility

For MRI systems, compatibility can be achieved by using nonmagnetic and nonconductive materials. For CT systems, radiolucency of the end-effector is important so that it can hold the instrument on the scan plane. The robot system must also be easily interfaced with the imaging system and allow quick access to the patient in emergency situations. When the

robot system is actuated it should not interfere with the imaging system. The kinematic structure of the robot must allow it to reach inside the gantry, which is one reason why specially designed robots are needed for these procedures.

### Registration

For a robot to target the anatomy based on the images, the coordinate system of the robot must be registered to the coordinate system of the imaging device. If the robot is permanently attached to the patient table of the imaging device, this registration can be done once through a calibration procedure. If the robot is designed to be moved from one imaging device to another or to be placed on the table for certain procedures, fast and accurate registration techniques are required.

### Patient movement and respiration

A limiting problem in some interventional techniques is organ movement due to respiration. High power robotic systems can react faster than a human and compensate for respiration and other movements (CyberKnife, Accuracy). This compensation would first require that target movement due to respiration be recognized and accurately tracked. However, for these systems to be clinically viable, robustness and safety are paramount.

### Force feedback

For robotic systems that include an active needle driver, at present there is no force feedback provided to the operator. The importance of this feedback is a subject of current debate but there are some clinical applications where it seems desirable. However, there is no accurate way to measure the force at the tip of surgical instruments and existing force feedback devices are too bulky for the clinical environment. In addition, friction forces on the cannula and tissue during insertion are high, which compromises the accuracy of force feedback measurements (27). Therefore, this topic must be considered a research issue at this time.

### Mode of control

The “best” user interface for an interventional robot has yet to be determined. For many procedures, joystick control seems well-suited and keeps the physician firmly in control. Master/slave systems are also possible and as noted above force feedback may be helpful here. However, there are procedures such as biopsy where a straight-line trajectory needs to be followed and some degree of autonomy seems appropriate if robustness can be achieved.

## Discussion and summary

As percutaneous procedures with cannulae and probes under image guidance continue to increase in numbers and importance, as they have the past several years, there will be more demand for technological assistance. In this role, image-guided robots may have a place and this place needs to be demonstrated in randomized clinical trials. Ten years ago image-guided procedures largely consisted of biopsies. Over the past decade interventional techniques have blossomed and include procedures to ablate tissue with energies such as radiofrequency, heat, cold, and laser. Reconstructive procedures have also developed. An example is vertebroplasty and kyphoplasty in which methymethacrylate is injected into vertebra under X-ray image guidance to increase stability and to reduce pain.

Robots have some potential advantages over the human operator in certain applications. Examples include working in hazardous environments such as imaging rooms where radiation is used. During fluoroscopic or CT guided procedures the operator frequently advances the cannula with the imaging beam off and then acquires additional images to identify the current position of the tip. Options to overcome the limitation of intermittent

imaging include stand-off devices to keep the operator's hands out of the direct x-ray beam. These devices are clumsy, and still force the operator to be too close to the radiation.

During percutaneous radiotherapy procedures radioactive seeds or probes are inserted into the patient. These are dangerous to have close to the operator. Other potential uses are to integrate robots with image guidance, including multimodality integration, and the integration of tracking technologies such as optical or mechanical trackers. The robots can perform active guidance in procedures where path planning and execution are difficult or provide a zone of constraint to keep the operator out of dangerous areas. A robot can also be integrated with active control to compensate for motion such as respiration. By compensating for patient motion the target can be made to appear static.

To be accepted in clinical practice, however, a robot must be intuitive and require minimal operator training. It must also be quick and easy to set up and not significantly increase the length of procedures. Robots must also be cost effective. The possibility of performing procedures that the human cannot perform but that are clinically necessary remains an ultimate goal for medical robotics. Engineers and physicians should work together to create and validate these systems for the benefits of patients everywhere.

## Acknowledgments

The Acubot and MRBot work was supported by U.S. Army grants DAMD17-99-1-9022 and W81XWH-04-1-007 and National Cancer Institute (NIH) grant CA088232.

The development of the prototype B-RobI was partly funded by the Austrian Federal Ministry of Transport, Innovation and Technology (BMVIT) and took place in cooperation with the Departments of Diagnostic Radiology and of Biomedical Engineering and Physics, Vienna University Hospital. Development of prototype B-RobII is a cooperation with Medical Intelligence GmbH, Schwabmünchen. The author (GK) would like to thank Joachim Kettenbach, Rudolf Hanel, Michael Figl, Wolfgang Birkfellner, Martin Fürst, Wolfgang Ptacek and Martin Kornfeld for their contributions.

The development of INNOMOTION, Innomedic, Herxheim, has been financially supported by the Forschungszentrum Karlsruhe, BASF Innovations Fonds, Ludwigshafen; tpg, Bonn; KfW, Frankfurt and WFT, Mainz, Germany. The animal trial has been performed at and supported by the Deutsches Krebsforschungszentrum DKFZ, Dept. of Medical Physics in Radiology, Heidelberg. The author (AM) would like to gratefully acknowledge the outstanding work and commitment of the teams:

- Innomedic, Herxheim
  - Andreas Berger, Andreas Lukoschek, Bernd Gutmann, Stephanie Gutmann, Lars Wischniewski, Horst Steigner, Thomas Remmele, Renate Wolf
- Research Center Karlsruhe:
  - Sandra Boscan, Heinz Becker, Helmut Breitwieser, Harald Fischer Lothar Gumb, Hartmut Gutzeit, Thomas Höhn, Heinz Junker, Marco Klein, Sven Köhn, Holger Krause, Martin Mark, Georg Prokott, Marco Sidor, Udo Voges, Oliver Wendt
- FH Gelsenkirchen
  - Peter Bremer, Thomas Bertsch, Waldemar Zylka
- St. Marien Hospital, Gelsenkirchen
  - Wolfram Triebe, Gert Lorenz
- Deutsches Krebsforschungszentrum DKFZ, Heidelberg
  - Michael Bock, Wolfhard Semmler
- University Heidelberg
  - Hamid Ghaderi, Hubertus Bardenheuer

## References

1. Craig, JJ. Introduction to Robotics. 2. Addison-Wesley; 1989.
2. Kwoh YS, Hou J, Jonckheere EA, Hayati S. A robot with improved absolute positioning accuracy for CT guided stereotactic brain surgery. IEEE Transactions on Biomedical Engineering. 1988; 35:153–60. [PubMed: 3280462]
3. Davies B. A review of robotics in surgery. Proc Inst Mech Eng [H]. 2000; 214:129–40.
4. Cleary K, Nguyen C. State of the art in surgical robotics: clinical applications and technology challenges. Comput Aided Surg. 2001; 6:312–28. [PubMed: 11954063]
5. Taylor RH, Stoianovici D. Medical robotics in computer-integrated surgery. Robotics and Automation. IEEE Transaction on Robotics and Automation. 2003; 19:765–81.
6. Pott PP, Scharf HP, Schwarz ML. Today's state of the art in surgical robotics. Comput Aided Surg. 2005; 10:101–32. [PubMed: 16298921]
7. Melzer A, Schurr MO, Kunert W, Buess G, et al. Intelligent Surgical Instrument System ISIS. Concept and Preliminary experimental application of components and prototypes. Endoscopic Surgery and Allied Technologies. 1993; 1:165–170. [PubMed: 8055318]
8. Guthart, GSJ.; Kenneth Salisbury, J. IEEE International Conference on Robotics and Automation. 2000. The intuitive telesurgery system: overview and application; p. 618-21.
9. Adler JR Jr, Murphy MJ, Chang SD, Hancock SL. Image-guided robotic radiosurgery. Neurosurgery. 1999; 44:1299–1306. discussion 1306–7. [PubMed: 10371630]
10. Stoianovici D, Cleary K, Patriciu A, Mazilu D, et al. AcuBot: A Robot for Radiological Interventions. IEEE Transactions on Robotics and Automation. 2003; 19:926–30.
11. Stoianovici, D.; Cadeddu, JA.; Demaree, RD.; Basile, SA.; Taylor, RH.; Whitcomb, LL.; Sharpe, WN.; Kavoussi, LR. An efficient needle injection technique and radiological guidance method for percutaneous procedures. In: Troccaz, J.; Grimson, E., editors. Computer Vision, Virtual Reality and Robotics in Medicine – Medical Robotics and Computer-Assisted Surgery (CVRMed-MRCAS'97). Grenoble, France: Springer-Verlag; 1997. p. 295-8.
12. Stoianovici, D.; Whitcomb, LL.; Anderson, JH.; Taylor, RH., et al. Medical Image Computing and Computer-Assisted Intervention. Springer-Verlag; 1998. A modular surgical robotic system for image guided percutaneous procedures; p. 404-10.
13. Patriciu, A.; Solomon, S.; Kavoussi, LR.; Stoianovici, D. Robotic Kidney and Spine Percutaneous Procedures Using a New Laser-Based CT Registration Method. In: Niessen, W.; Viergever, MA., editors. Medical Image Computing and Computer-Assisted Intervention. Utrecht, Netherlands: Springer-Verlag; 2001. p. 249-58.
14. Solomon SB, Patriciu A, Bohlman ME, Kavoussi LR, et al. Robotically Driven Interventions: A Method of Using CT Fluoroscopy without Radiation Exposure to the Physician. Radiology. 2002; 225:277–82. [PubMed: 12355016]
15. Cleary K, Stoianovici D, Patriciu A, Mazilu D, et al. Robotically assisted nerve and facet blocks: a cadaveric study. Academic Radiology. 2002; 9:821–5. [PubMed: 12139100]
16. Kronreif G, Fürst M, Kettenbach J, Figl M, et al. Robotic guidance for percutaneous interventions. Advanced Robotics. 2003; 17:541–60.
17. Kronreif, G.; Kettenbach, J.; Figl, M.; Kleiser, L., et al. Computer Assisted Radiology and Surgery (CARS). Elsevier; 2004. Evaluation of a robotic targeting device for interventional radiology; p. 486-91.
18. Kettenbach J, Kronreif G, Figl M, Furst M, et al. Robot-assisted biopsy using computed tomography-guidance: initial results from in vitro tests. Invest Radiol. 2005; 40:219–28. [PubMed: 15770140]
19. Kettenbach J, Kronreif G, Figl M, Furst M, et al. Robot-assisted biopsy using ultrasound guidance: initial results from in vitro tests. Eur Radiol. 2005; 15:765–71. [PubMed: 15449006]
20. Korb W, Kornfeld M, Birkfellner W, Boesecke R, et al. Risk analysis and safety assessment in surgical robotics: A case study on a biopsy robot. Min Invas Ther & Allied Technol. 2005; 14:23–31.
21. Melzer A, Seibel R. MR guided therapy of spinal disease. Min Invas Ther & Allied Technol. 1999:89–93.

22. Melzer A, Gutmann B, Lukoschek A, Mark M, et al. Experimental Evaluation of an MRI compatible Telerobotic System for CT MRI guided Interventions. Supplement to Radiology. 2003; 226:409–#444.
23. Bock M, Zimmerman H, Gutmann B, Melzer A, et al. Combination of a Fully MR-compatible Robotic Assistance System for Closed-bore High-field MRI Scanners with Active Device Tracking and Automated Image Slice Positioning. Radiological Society of North America Scientific Program, Supplement to Radiology. 2004; 227:398.
24. Stoianovici D, Patriciu A, Mazilu D, Petrisor D, et al. Multi-Imager Compatible Robot for Transperineal Percutaneous Prostate Access. IEEE Transactions on Robotics. 2005 submitted.
25. Stoianovici D, Patriciu A, Mazilu D, Petrisor D, et al. Pneumatic Step Motor. IEEE/ASME Transactions on Mechatronics. 2005 submitted.
26. Stoianovici D. Multi-Imager Compatible Actuation Principles in Surgical Robotics. International Journal of Medical Robotics and Computer Assisted Surgery. 2005; 1:86–100. [PubMed: 17518382]
27. Breitwieser H, Boscan SM, Becker H, Voges U, et al. Feasibility of Manual Control Device for Robotic Assisted Needle Insertion in CT and MRI. Supplement to Radiology. 2002; 225:155–192VI.

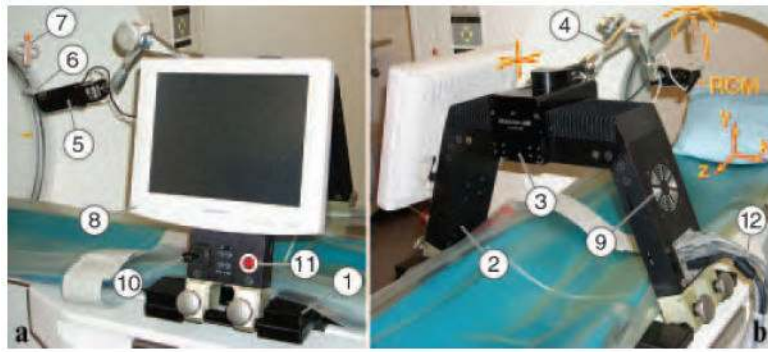


**Figure 1.**  
Front (a) and side (b) views of the AcuBot.

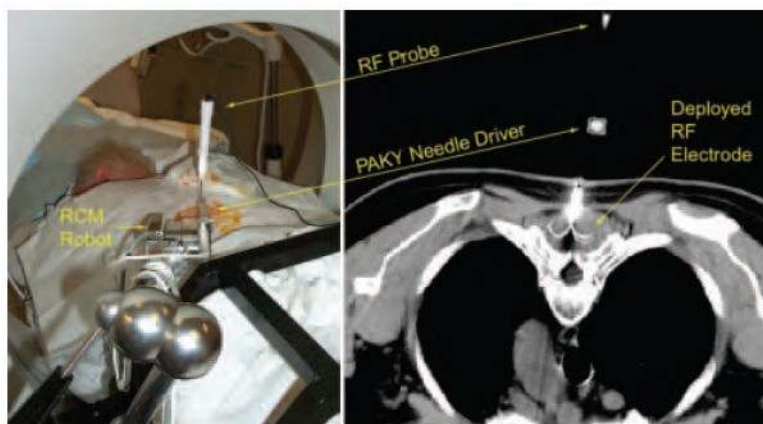


**Figure 2.** CT-guided RF ablation with PAKY-RCM system and laser-based registration.

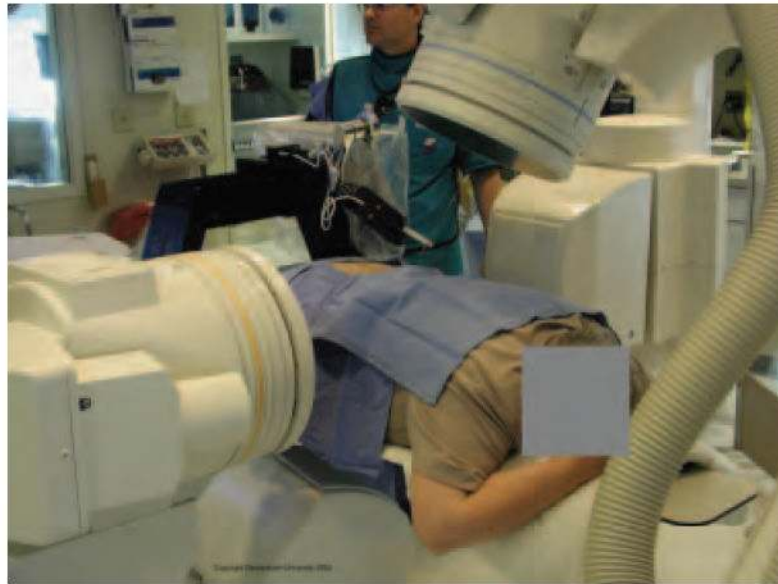


**Figure 3.** Clinical trial of robotically assisted nerve blocks at Georgetown University under biplane fluoroscopy.





**Figure 4.**  
Biopsy robot I during *in vitro* testing for image-guided interventions under CT fluoroscopy.



**Figure 5.** Close-up of testing showing phantom (peas can be seen in the bag), needle positioning unit (NPU), and optical trackers.



**Figure 6.**  
Biopsy robot II in a 2 by 2 degree of freedom configuration mounted on two passive holding arms.



**Figure 7.**  
Biopsy robot II during initial phantom study.



**Figure 8.**  
(a) INNMOTION robot for MRI-guided procedures; (b) moved into the bore.

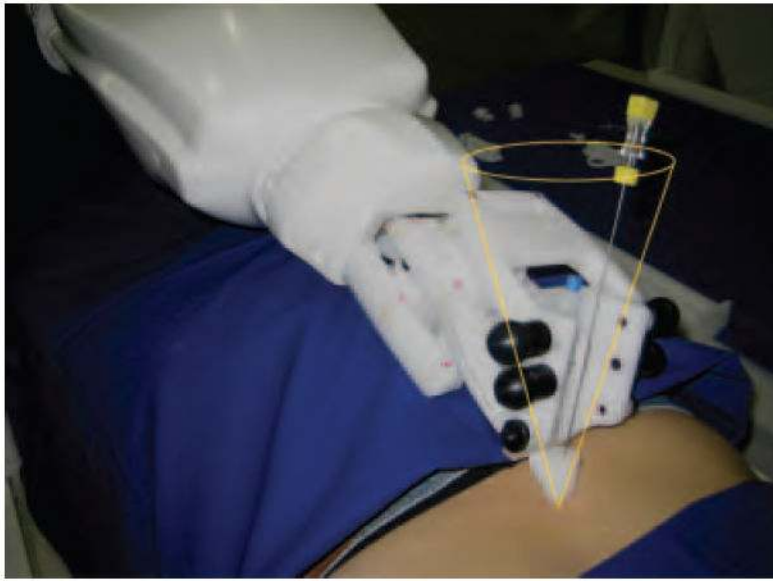


**Figure 9.**  
Application module for manual cannula insertion.



**Figure 10.** INNOVATION with six degrees of freedom can be mounted on different types of MRI patient beds.

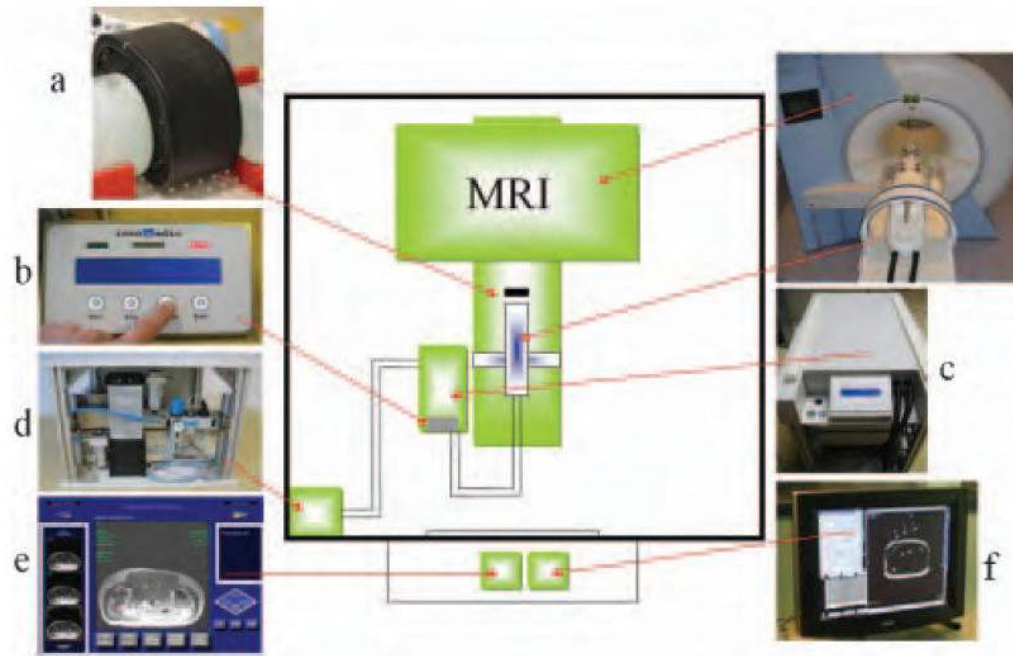


**Figure 11.** Equipment setup (a) target phantom, (b) input panel, (c) in room control unit, (d) pneumatic unit, (e) graphical user interface, and (f) MRI console monitor.



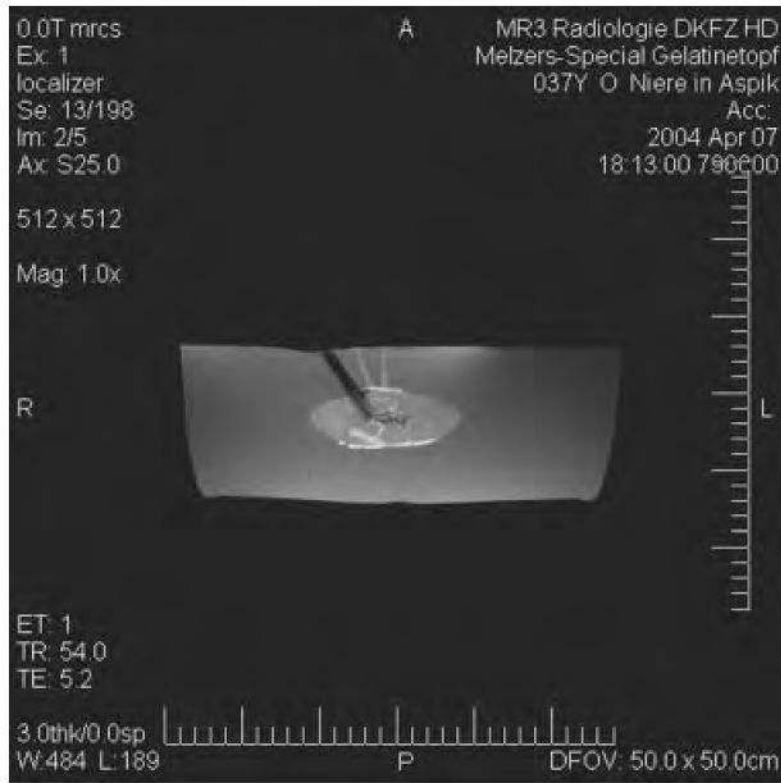


**Figure 12.** MRI target precision of 20 Gauge cannula insertion into a porcine kidney embedded in Agarose.



**Figure 13.** Overlay images on the INNOMOTION screen for evaluation of target precision.



**Figure 14.** MR compatible robot developed for prostate brachytherapy at Johns Hopkins (simulation of a clinical procedure).



**Figure 15.**  
A 4x4 pattern of seeds with 10 mm spacing automatically placed in agar shows average seed placement errors of 0.652 mm.

**Table 1**

The four interventional robot systems described in this article.

<b>System</b>	<b>Institution</b>	<b>Status</b>	<b>Imaging Modality</b>
AcuBot	Hopkins/Georgetown (USA)	Cadaver studies Animal studies Clinical trial done	Fluoroscopy and CT
B-Rob	ARC Seibersdorf research (Austria)	Phantom studies	CT and ultrasound
INNOMOTION	Innomedic/FZK/FH Ge (Germany)	Animal studies Clinical use starting CE marked	MRI and CT
MR Bot	Hopkins (USA)	Phantom studies	MRI